A. 研究目的

Troglitazone (TRO) is one of the thiazolidinedione (TZD) oral antidiabetic agents launched in 1997. This drug has been demonstrated to improve hyperglycemia, hyperinsulinemia, and hypertriglyceridemia as well as to ameliorate the insulin sensitivity of the target tissues (Fujiwara et al., 1988; Nolan et al., 1994). Based on its pharmacological advantages and the apparent absence of severe toxic effects, TRO was thought likely to become a promising treatment for type II diabetes mellitus in patients with insulin resistance. However, in the early clinical trials, 1.9% of the patients who received TRO experienced an elevation of serum alanine aminotransferase of more than 3 times the normal upper limit (Watkins and Whitcomb, 1998). During the following few years of utilization, TRO had been reported to produce idiosyncratic hepatotoxic effects in some individuals (Gitlin et al., 1998; Neuschwander-Tetri et al., 1998; Shibuya et al., 1998). Because of the seriousness of the cases, TRO was considered for withdrawal from the market in 2000. The mechanism by which TRO induced toxicity is still not completely understood. Severe hepatotoxic effects have not been observed in any kind of conventional animal models including monkey, which has a similar metabolic profile to human (Rothwell et al., 2002; Watanabe et al., 1999).

The antidiabetic effects of TZDs occur via the activation of peroxisome proliferator-activated receptor g (PPARg), and the potency correlates to their receptor-binding activities (Lehmann et al., 1995). There is a less clear association between hepatotoxicity and rosiglitazone (RSG), another TZD agent (Freid et al., 2000; Isley and Oki, 2000; Lebovitz et al., 2002). Since hepatotoxicity is unique to TRO, it is unlikely to be related to a PPARg class effect.

Even though TRO toxicity has not been observed in *in vivo* experimental animal studies, a number of *in vitro* experiments revealed evidence that TRO can cause apoptotic cell death in various hepatic cell types (Bae and Song, 2003; Tirmenstein et al., 2002; Yamamoto et al., 2001). The degree of lethality also depends on the concentration of the agent and the duration of exposure. Tirmenstein et al. (2002) reported that TRO induces mitochondria permeability transition and decreases in the cellular ATP concentration prior to cell death. Regarding the signaling pathway of apoptosis, Bae and Song (2003) reported that TRO but not RSG activates both c-Jun N-terminal protein kinase (JNK) and p38 kinase and causes an increase in proapoptotic proteins such as Bad and Bax, release of cytochrome c and cleavage of Bid, together with a decrease in antiapoptotic protein, Bcl-2.

In addition to the known mechanisms of apoptotic cell death caused by TRO, this study investigated the involvement of proteins whose up- or down-regulation correlated with the TRO-induced toxic effects. Using a proteomic analysis strategy, a protein spot on a gel separated by 2-dimensional

electrophoresis (2-DE) at an approximate molecular weight (MW) of 75 kDa and isoelectric point (pI) of 5 was analyzed. This spot was increased greatly in correlation with the concentration-dependent exposure to TRO. The protein was identified as a mixture of two chaperones, immunoglobulin heavy chain binding protein (BiP or Grp78) and, to a lesser extent, protein disulfide isomerase related protein (PDIrp or ERp72). These findings suggest that TRO targets the endoplasmic reticulum (ER) and causes the overexpression of BiP, a prominent chaperone, in response to cytotoxicity. A possible association of BiP in TRO-induced cytotoxicity is also discussed.

B. 研究方法

B-1. Cell culture condition and treated agents

Human hepatoma cell lines HepG2 and HLE were obtained from the Riken Gene Bank (Tsukuba, Japan) and the Japanese Collection of Research Biosources (Tokyo, Japan), respectively. The cells were maintained in Dulbecco's Modified Eagle's Medium (DMEM, Nissui Pharmaceutical, Tokyo, Japan) containing 10% fetal bovine serum (FBS, BioWhitaker, Walkersville, MD) at 37°C in a humidified atmosphere with 5% CO_2. TRO and RSG were kindly provided by Sankyo (Tokyo, Japan). The treated agents were dissolved in dimethyl sulfoxide (DMSO, Wako, Osaka, Japan), in which the final concentration did not exceed 0.1%. In all treatment conditions, the cells were grown in medium containing 5% FBS.

B-2. Cytotoxicity assay

To assess the cytotoxicity, a crystal violet assay and an ATP-based luminescent assay were used. Crystal violet assay was used according to Nakagawa et al. (1996) for determining the concentration- and time-dependent toxicity in HepG2 cells. Briefly, a suspension of HepG2 cells ($1x10^5$ cells/well) in the presence of TZDs or 0.1 % DMSO was seeded onto 12-well plates. At the end of treatment, adherent cells were washed 3 times with phosphate buffered saline (PBS), fixed with 3.7% formaldehyde and stained with 0.2% crystal violet. The absorbance at 620 nm was measured after extracting the cells with 2% sodium dodecyl sulfate (SDS). Percent cell viabilities were calculated by comparing them to the absorbance of 0.1% DMSO-treated cells.

Cell viabilities based on the quantity of the ATP produced by metabolically active cells were assessed with a CellTiter-Glo Luminescent assay kit (Promega, Madison, WI) according to the manufacturer's protocol. In the concentration-dependent study, a suspension of HepG2 cells ($3x10^3$cells/well) in the presence of TZDs or 0.1 % DMSO was seeded onto a 96-well plate. At the end of treatment, CellTiter-Glo reagent was added at an equal volume to the cell culture medium present in each well. The generated luminescent signal was monitored on a Wallac 1420 multilabel counter (PerkinElmer, Wellesley, MA).

B-3. Preparing cell lysates

HepG2 cells were treated with various doses of TRO or RSG. At the end of the 48 h treatment period, the cells were harvested by treatment with 0.05% trypsin plus 0.02% EDTA. The cells were washed with PBS and lysed with 100-200 μl of lysis solution (8 M urea, 4% CHAPS, 2% Pharmalyte 3-10) containing protease inhibitors (1 mM DTT, 0.5 mM APMSF, 2 μg/ml aprotinin, 2 μg/ml pepstatin and 2 μg/ml leupeptin). The cell suspension was centrifuged at 12,000 rpm for 1 h to remove cell debris. The supernatant was collected and the protein concentration was measured using a Bio-Rad Protein Assay Kit (Bio-Rad Laboratories, Hercules, CA). The cell lysates were stored at -80°C until the time of analysis.

B-4. 2-Dimensional electrophoresis (2-DE)

The devices and chemicals used in 2-DE were purchased from Amersham Biosciences, Buckinghamshire, UK. For the first dimension, 500 μg of protein of the cell lysates was mixed with Destreak Rehydration Solution containing immobilized pH gradient (IPG) buffer of pH 4-7 and applied onto IPG gel strips. The samples were rehydrated at 20°C for 14 h and subsequently separated at 17,500 V-h using an Ettan IPGphor Isoelectric Focusing System. The second dimensional electrophoresis was run on 10% acrylamide gel at 10°C for 4 h. The separated proteins on 2-DE were visualized by Coomassie brilliant blue (CBB) staining.

B-5. Protein identification

The amino acid sequence analyses from the CBB stained 2-dimensional (2-D) gels were performed at Hitachi Science Systems, Ltd., Japan. The protein spot of interest was excised from the CBB stained gel of the sample treatment with 75 μM TRO. After in-gel digestion with trypsin, the peptides were reduced and carbamidomethylated. The peptide mass mapping was performed on an ESI-TRAP and analyzed by LC/MS/MS. The matched peptides were searched using MASCOT (http://www.matrixscience.co.uk) based on the NCBInr database.

B-6. Western blotting

The HepG2 cell lysates (50 μg for BiP, and 25 μg proteins for PDIrp and PDI proteins) were separated on 10% SDS-polyacrylamide gels and transferred onto PVDF membrane (Immobilon-P, Millipore, Billerica, MA). The specific proteins were detected by mouse anti-KDEL monoclonal antibody (SPA-827, Stressgen, San Diego, CA) for BiP, rabbit anti-ERp72 polyclonal antibody (SPA-720, Stressgen) for PDIrp, and rabbit anti-PDI polyclonal antibody (SPA-890, Stressgen) for PDI proteins at dilutions of 1:200, 1:2000 and 1:2000, respectively. The protein bands were developed by biotinylated second antibody-peroxidase reaction. The quantitative analysis of protein expression was performed using a densitometer GS-700 (Bio-Rad Laboratories).

B-7. Reverse transcription and real-time PCR

Human hepatoma cells were treated with or without TZDs. At the end of the incubation periods, the cells were washed with PBS and the total RNA was prepared using Isogen® (Nippon Gene, Tokyo, Japan) according to the manufacturer's instructions. Reverse transcription (RT) reactions were carried out by incubating 2 μg of total RNA with random primer (Takara, Tokyo, Japan) and Moloney-Murine Leukemia Virus Reverse transcriptase (M-MLV-RT) RNaseH Minus (Toyobo, Tokyo, Japan) at 37°C for 1 h. Subsequently, the steady state of the mRNA levels was quantified by fluorescence-based real-time PCR. Oligonucleotide sense and antisense primers of human-BiP (5'-TGCTTGATGTATGTCCCCTTA-3' and 5'-CCTTGTCTTCAGCTGTCACT-3') and PDIrp (5'-AATACCAGGATGCCGCTAAC-3' and 5'-GCAAAGGTGTACTCAGGGAA-3') as well as GAPDH (5'-CCAGGGCTGCTTTTAACTC-3' and 5'-GCTCCCCCCTGCAAATGA-3') were used. The reaction mixture for real-time PCR containing 1 μl of RT product, *Ex Taq* R-PCR Version (Takara, Japan), SYBR® Green I (Molecular Probes, Eugene, OR) and the specific sense and antisense primers were subjected to a Smart Cycler® System (Cepheid, Sunnyvale, CA). After a holding step at 95°C for 30 s, the thermal cycling was repeated for 45 cycles of 94°C for 4 s and 64°C for 20 s followed by melting from 60°C to 95°C at 0.2°C/s. The standard curve for the relative quantification was created by serially diluted GAPDH concentrations plotted against the threshold cycle number from the real-time PCR reaction. The BiP and PDIrp expressions were evaluated, and the relative values were normalized with the GAPDH values from the same DNA samples.

B-8. siRNA generation

Small interference RNA (siRNA) for BiP (Accession AF188611) and human lamin A (Accession X03444) mRNA target sequences were created and checked by the species-appropriate genome database (http://www.ncbi.nlm.nih.gov/BLAST/) to avoid target sequences homologous to other known coding sequences. The sense and antisense primers for BiP were 5'-CAACTGTTACAATCAAGGTC-3' and 5'-CTGTATCCTCTTCACCAGTT-3', and for lamin A were 5'-AAAGCGCGCAATACCAAGAA-3' and 5'-CCTCACTGTAGATGTTCTTC-3', designed with the T7 RNA polymerase promoter sequences (CTAATACGACTCACTATAGGGAGG) at the 5'-end of each primer. The target genes were amplified by PCR and purified by ethanol precipitation. dsRNAs were generated using a T7 RiboMAX™ Express Large Scale RNA Production System Kit (Promega) according to the manufacturer's protocol. The dsRNAs were then diced into 20-23 bp of siRNAs by incubating them with recombinant dicer enzyme (GTS, San Diego, CA) for 18 h. The obtained siRNAs were further subjected to two purification steps, removal of the salts

with a Sephadex G25 column (Amersham Biosciences) and the undigested dsRNA by centrifugation with a Microcon YM-100 (Millipore). The purified siRNA duplexes were stored at -80°C until analysis.

B-9. Transfection of siRNA

In order to knockdown target genes at the transcriptional level, siRNA was transfected into the cells. Because of the difficulty to transfect siRNA into HepG2 cells, HLE cells, another human hepatoma cell line which demonstrates similar BiP expression profiles to HepG2 cells (data not shown), were used in this experiment. Briefly, HLE cells were seeded onto 6-well plates ($8x10^4$ cells/well) or 96-well plates ($3x10^3$ cells/well) and incubated for 24 h before transfection. At approximately 30-50% confluency, the cells were transfected with siRNA using Oligofectamine (Invitrogen, Carlsbad, CA) for 24 h. The cells were treated with TZDs or DMSO at the concentrations indicated for 24 h before analysis.

B-10. Statistical analysis

Data were analyzed by one-way analysis of variance (ANOVA) followed by Dunnett's post hoc test using Instat version 2.0 software. $p < 0.05$ was considered significant.

C. 実験結果

C-1. Troglitazone-induced HepG2 cell toxicity

To investigate the toxic effects of TRO, crystal violet assay was used to determine the concentration- and time-dependent cytotoxicity. ATP-based luminescent assay was used for the sensitive detection of a small amount of viable cells. In the concentration-dependent experiment, HepG2 cells were exposed to various concentrations of TRO ranging from 0 (0.1% DMSO), 5, 10, 25, 50, 75 and 100 μM as well as the same concentrations of RSG as negative controls. After 48 h of treatment, ≥ 25 μM TRO significantly reduced the cell viability with an approximate IC_{50} of 40 μM, whereas RSG showed no significant toxic effects (Fig. 1A). TRO also showed a time-dependent cytotoxicity in HepG2 cells from 24 to 60 h of exposure ($p < 0.01$) compared to the DMSO treatment (Fig. 1B). The concentration-dependent cytotoxicity of TRO (Fig. 1A) was comparable to the reduction of ATP produced by viable metabolically active cells as detected by the ATP-based luminescent assay (Fig. 1C).

C-2. Proteomic analysis for troglitazone-induced hepatotoxicity

The different toxic effects of TRO and RSG were investigated by proteomic analysis to determine the differences in the protein expression profiles. HepG2 cells were treated with or without various doses of TRO or RSG for 48 h. Cell lysates were prepared and subjected to 2-DE analysis. The gels were then stained with CBB. We focused on the spot showing a large amount of protein expression which showed dose-dependent and TRO-specific changes at an approximate MW of 75 kDa and isoelectric point of 5.0. The

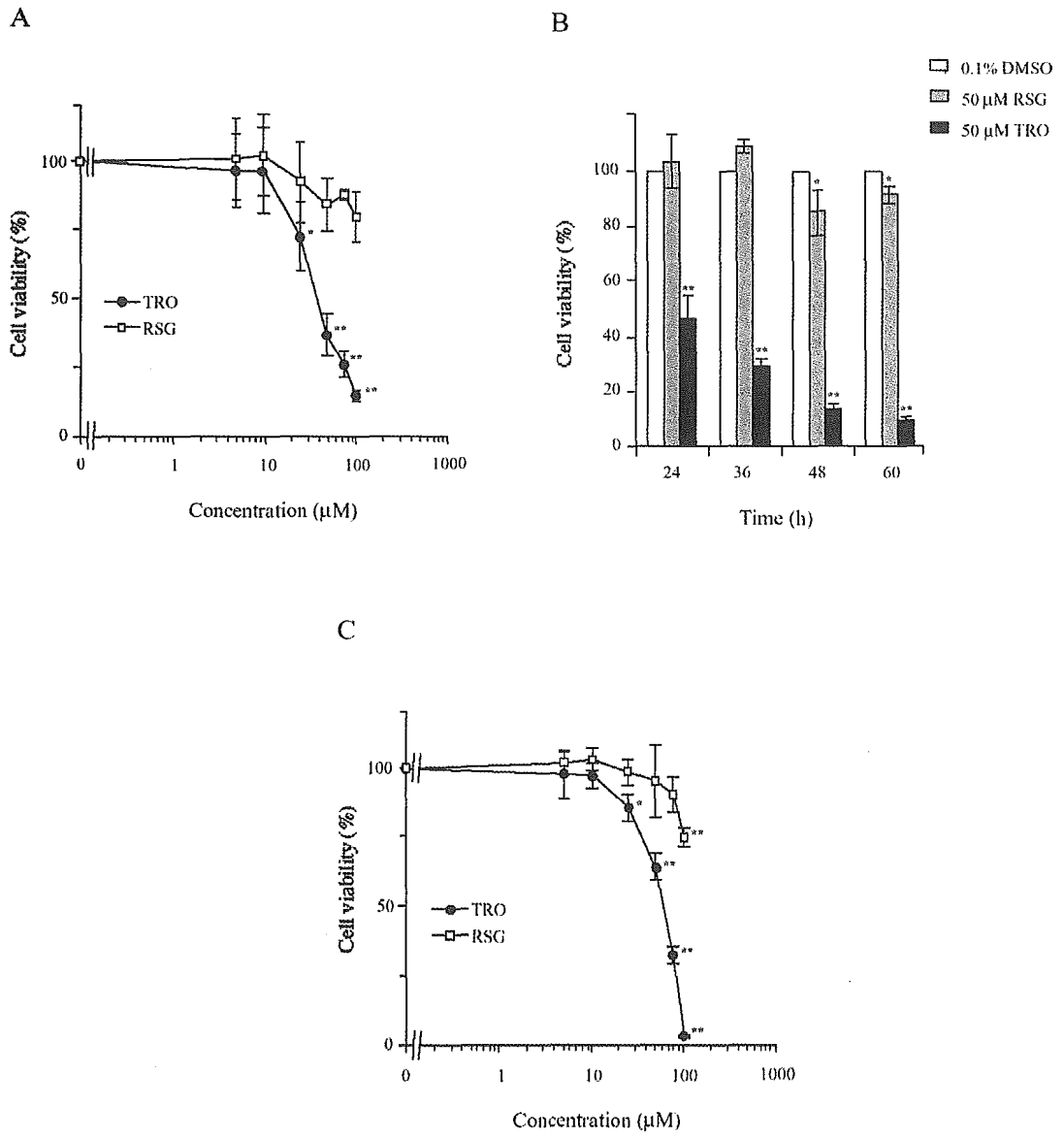

Fig. 1. TZDs cytotoxicity in HepG2 cells. A, HepG2 cells were incubated with 0.1% DMSO (control) or the indicated concentration of TRO or RSG for 48 h. B, HepG2 cells were incubated with 0.1% DMSO (control) or 50 μM TZDs for the indicated time. Cell viabilities were assessed by crystal violet assay. C, HepG2 cells were incubated with 0.1% DMSO (control) or the indicated concentration of TRO or RSG for 48 h. Cell viabilities were measured by ATP-based luminescent assay. The results represent the mean ± SD of at least three independent experiments. * $p < 0.05$, ** $p < 0.01$ compared with the control.

expression was increased by treatment with 50 and 75 μM of TRO (Fig. 2A). At the same position, RSG treated cells demonstrated no difference compared to the DMSO-treated control (Fig. 2B).

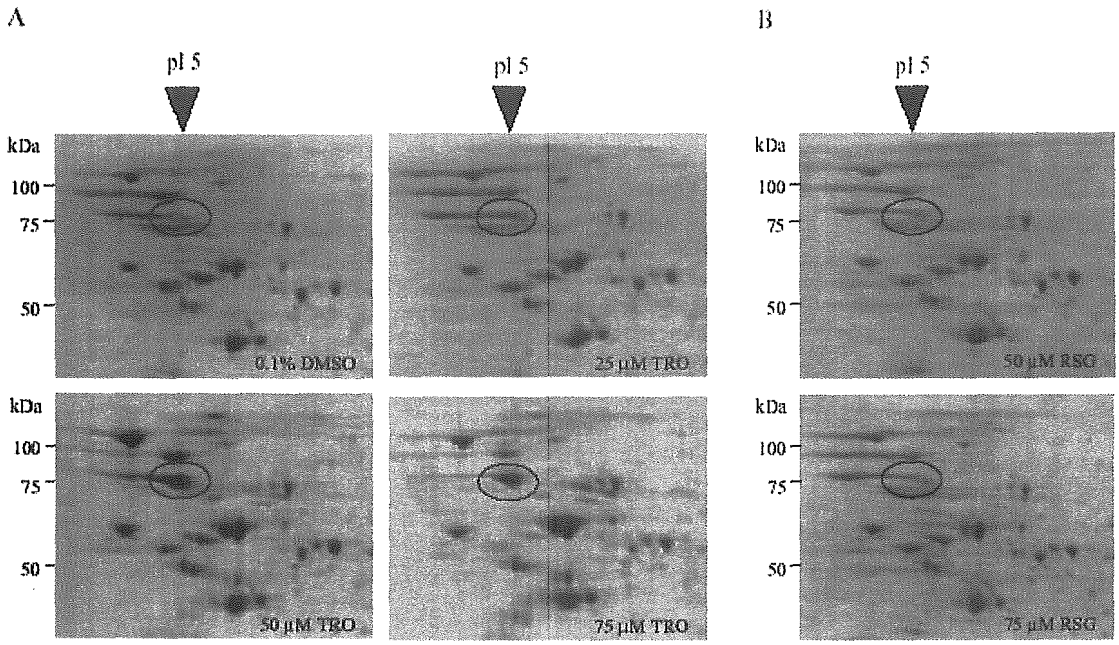

Fig. 2. Protein expression profiles of 2-D gels from CBB staining. HepG2 cells were incubated with 0.1% DMSO (control) or the indicated concentration of TRO or RSG for 48 h. The cell lysates were separated by 2-DE and stained with CBB. The oval frames mark the proteins of interest which increased in a concentration-dependent manner by TRO treatment.

The spot was excised, subjected to amino acid sequence analysis and identified as a mixture of immunoglobulin heavy chain binding protein (BiP) (Fig. 3A) and, to a lesser extent, protein disulfide isomerase related protein (PDIrp or ERp72) (Fig. 3B). Notably, BiP was prominent in this finding as indicated by the higher total score (1341) compared to PDIrp (294) and these proteins had MWs and calculated isoelectric point values near the position that appeared on the 2-D gels.

C-3. Changes of chaperone proteins and mRNAs by TZDs exposure

HepG2 cells were incubated in the presence of various concentrations of TRO or RSG or 0.1% DMSO (control) for 48 h. The cell lysates were confirmed for the expressions of BiP and PDIrp proteins by Western blotting with specific antibodies. In Fig. 4A, BiP protein detected by anti-KDEL antibody was markedly increased in intensity by increasing the TRO concentration and was about 5-fold at 100 μM. The same phenomenon was also demonstrated with RSG treatment but with a relatively smaller increase, even at 100 μM (about 2.5-fold). The expression of PDIrp as detected by anti-ERp72 antibody showed no significant difference among the treatments (Fig. 4B). The expression of PDI protein was also investigated and there was no significant difference (Fig. 4C).

A

BiP

gi|6470150; Total score: 1341
BiP protein [Homo sapiens]
Nominal mass (Mr): 71002
Calculated pI: 5.23

```
  1 MEEDKKEDVG TVVGIDLGTT YSCVGVFKNG RVEIIANDQG NRITPSYVAF TPEGERLIGD
 61 AAKNQLTSNP ENTVFDAKRL IGRTWNDPSV QQDIKFLPFK VVEKKTKPYI QVDIGGGQTK
121 TFAPEEISAM VLTKMKETAE AYLGKKVTHA VVTVPAYFND AQRQATKDAG TIAGLNVMRI
181 INEPTAAAIA YGLDKREGEK NILVFDLGGG TFDVSLLTID NGVFEVVATN GDTHLGGEDF
241 DQRVMEHFIK LYKKKTGKDV RKDNRAVQKL RREVEKAKRA LSSQHQARIE IESFYEGEDF
301 SETLTRAKFE ELNMDLFRST MKPVQKVLED SDLKKSDIDE IVLVGGSTRI PKIQQLVKEF
361 FNGKEPSRGI NPDEAVAYGA AVQAGVLSGD QDTGDLVLLD VCPLTLGIET VGGVMTKLIP
421 RNTVVPTKKS QIFSTASDNQ PTVTIKVYEG ERPLTKDNHL LGTFDLTGIP PAPRGVPQIE
481 VTFEIDVNGI LRVTAEDKGT GNKNKITITN DQNRLTPEEI ERMVNDAEKF AEEDKKLKER
541 IDTRNELESY AYSLKNQIGD KEKLGGKLSS EDKETMEKAV EEKIEWLESH QDADIEDFKA
601 KKKELEEIVQ PIISKLYGSA GPPPTGEEDT AELHHHHHH
```

B

PDIrp

gi|4758304; Total score: 294
Protein disulfide isomerase related protein
(calcium-binding protein, intestinal-related) [Homo sapiens]
Nominal mass (Mr): 73229
Calculated pI: 4.96

```
  1 MRPRKAFLLL LLLGLVQLLA VAGAEGPDED SSNRENAIED EEEEEEEDDD EEEDDLEVKE
 61 ENGVLVLNDA NFDNFVADKD TVLLEFYAPW CGHCKQFAPE YEKIANILKD KDPPIPVAKI
121 DATSASVLAS RFDVSGYPTI KILKKGQAVD YEGSRTQEEI VAKVREVSQP DWTPPPEVTL
181 VLTKENFDEV VNDADIILVE FYAPWCGHCK KLAPEYEKAA KELSKRSPPI PLAKVDATAE
241 TDLAKRFDVS GYPTLKIFRK GRPYDYNGPR EKYGIVDYMI EQSGPPSKEI LTLKQVQEFL
301 KDGDDVIIIG VFKGESDPAY QQYQDAANNL REDYKFHHTF STEIAKFLKV SQGQLVVMQP
361 EKFQSKYEPR SHMMDVQGST QDSAIKDFVL KYALPLVGHR KVSNDAKRYT RRPLVVVYYS
421 VDFSFDYRAA TQFWRSKVLE VAKDFPEYTF AIADEEDYAG EVKDLGLSES GEDVNAAILD
481 ESGKKFAMEP EEFDSDTLRE FVTAFKKGKL KPVIKSQPVP KNNKGPVKVV VGKTFDSIVM
541 DPKKDVLIEF YAPWCGHCKQ LEPVYNSLAK KYKGQKGLVI AKMDATANDV PSDRYKVEGF
601 PTIYFAPSGD KKNPVKFEGG DRDLEHLSKF IEEHATKLSR TKEEL
```

Fig. 3. Amino acid sequences analyzed from the 2-D gel spot. The protein spot of interest was excised from the CBB stained gel of the sample treated with 75 μM TRO and subjected to amino acid sequence analyses as described in Experimental Procedures. The 'Bold red' sequences denote peptides which matched with both BiP (A) and PDIrp (B).

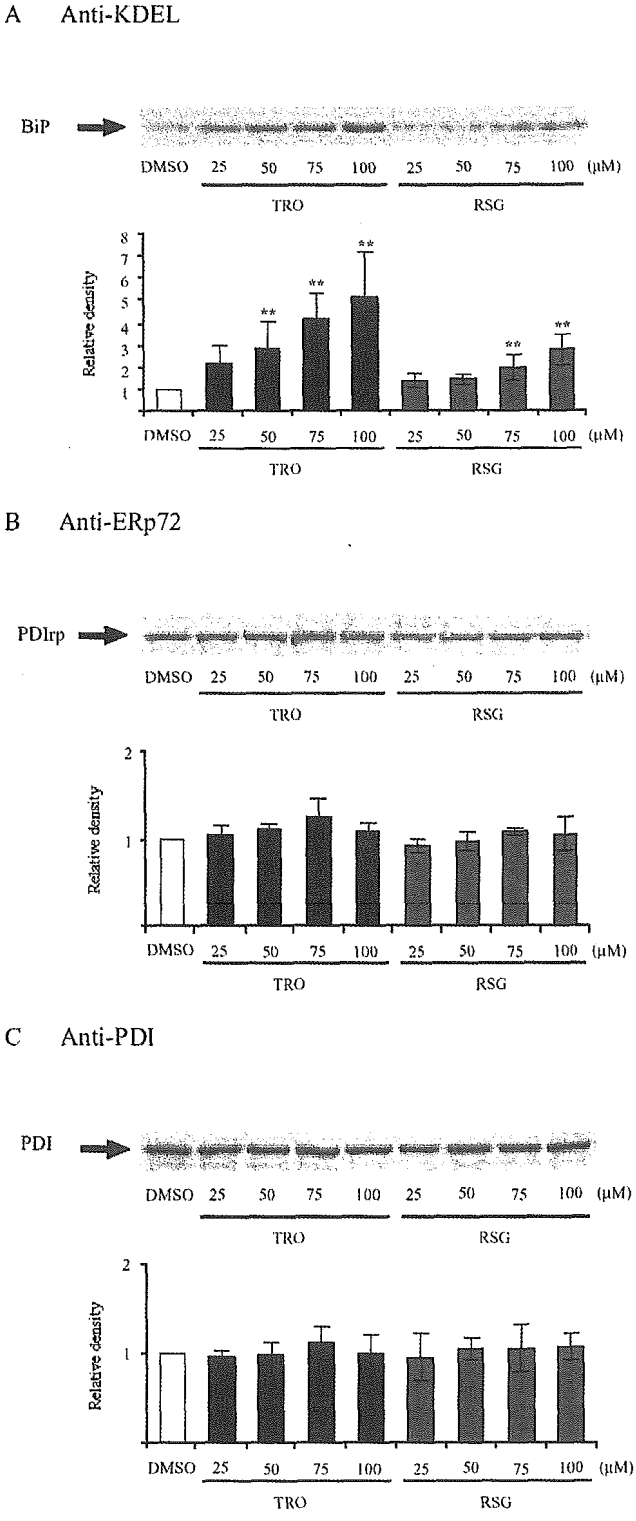

Fig. 4. Changes of BiP, PDIrp and PDI protein expression by TZDs in HepG2 cells. HepG2 cells were incubated with 0.1% DMSO (control) or the indicated concentrations of TRO or RSG for 48 h. The cell lysates were subjected to Western blotting with mouse anti-KDEL (A), rabbit anti-ERp72 (B) and rabbit anti-PDI (C) antibodies for BiP, PDIrp and PDI proteins, respectively. Two additional studies yielded equivalent results. The expressions of BiP, PDIrp and PDI proteins were measured using a densitometer. The data represent the mean ± SD of three independent experiments. ** $p < 0.01$ compared with the control.

To further investigate the control of BiP and PDIrp expressions at the transcription level, the mRNAs were determined by real-time PCR. Comparing the results from the Western blotting, BiP mRNA expression by TRO treatment was also dose-dependently induced, with the highest level at 75 μM (about 11-fold) (Fig. 5A). However, at 100 μM of TRO, BiP mRNA was comparable to the control because of cell toxicity. RSG treated cells showed a small tendency to increase, with significance at the higher doses of 75 and 100 μM (Fig. 5A). Although PDIrp protein was equally expressed in the presence of all treatments, mRNA expression in response to TRO and RSG treatment showed the induction at the doses of 75 and 100 μM (Fig. 5B).

C-4. Inhibition of BiP expression by siRNA

All the above results demonstrated the obvious effects of TRO compared to RSG on BiP overexpression. To clarify these effects, an RNA interference technique was carried out for knockdown BiP expression. Because of the difficulty in transfecting siRNA into HepG2 cells, human hepatoma HLE cells were used instead. In previous report, TRO possessed toxic effects on HLE cells as well as HepG2 cells, but with somewhat higher sensitivity (Yamamoto et al., 2001). The BiP mRNA expression in HLE cells treated with

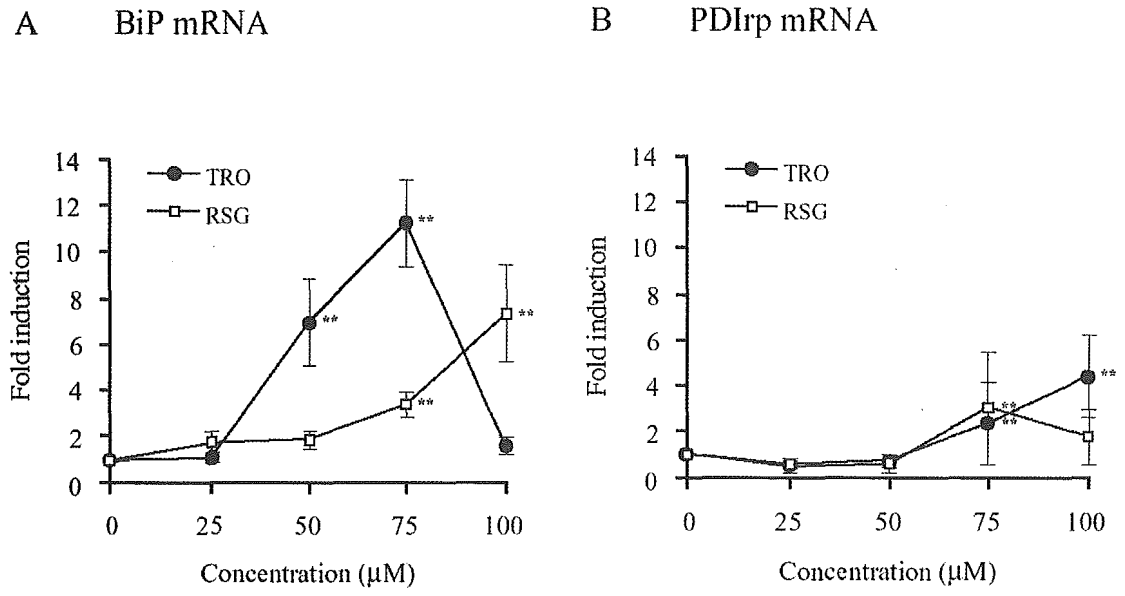

Fig. 5. Changes of BiP and PDIrp mRNA expression by TZDs in HepG2 cells. HepG2 cells were incubated with 0.1% DMSO (control) or the indicated concentrations of TRO or RSG for 48 h. The cDNA were prepared for real-time PCR. Sense and antisense primers of BiP (5'-TGCTTGATGTATGTCCCCTTA-3' and 5'-CCTTGTCTTCAGCTGTCACT-3') and PDIrp (5'-AATACCAGGATGCCGCTAAC-3' and 5'-GCAAAGGTGTACTCAGGGAA-3') were used. The relative BiP and PDIrp expression values were normalized with the GAPDH values of the same samples. The data represent the mean ± SD of three independent experiments. ** $p < 0.01$ compared with the control.

TRO and RSG showed a similar pattern to that in HepG2 cells (data not shown). Compared to mock-transfected cells, BiP expression with DMSO treatment (control) was diminished by 50 and 100 nM of siRNA by about 30% and 17%, respectively. Furthermore, when additionally treated with 75 μM of TRO, the BiP mRNA was dramatically suppressed from 16-fold to 1.7- and 1.6-fold, respectively (Fig. 6A). Similarly, in siRNA-transfected cells treated with 100 μM of RSG, the BiP mRNA was suppressed from 2.5-fold to 0.6- and 1.0-fold, respectively (Fig. 6A). The BiP protein expression was also investigated in HLE cells after transfection with 50 nM BiP siRNA and subsequent treatment with TRO and RSG at concentrations of 75 and 100 μM, respectively. Fig. 6B shows the inhibition of BiP protein production compared to the mock-transfected control under both control (DMSO) and treatment conditions assessed by Western blotting.

C-5. Cell viability changes by troglitazone treatment in BiP suppressed cells

BiP inhibition by siRNA was clearly demonstrated, especially in the presence of TRO and RSG, to be superior to that of the mock-transfected control. Accordingly, HLE cells were then investigated in terms of the phenotypic changes. The ATP-based luminescent assay was used to measure the cell viability. In the DMSO-treated control there was a dose-dependent decrease in cell viability by BiP siRNA transfection (Fig. 7A) whereas there were no significant changes by lamin A siRNA, a negative control of siRNA transfection (Fig. 7B). Interestingly, 50 μM TRO treatments caused a significant decrease in cell viability with 10 nM of BiP siRNA ($p < 0.05$) and a marked decreased ($p < 0.01$) at the high concentration of 25 to 100 nM of BiP siRNA compared to the DMSO-treated control (Fig. 7A). The 75 μM TRO treatment demonstrated significant toxic effects ($p < 0.01$) in all BiP siRNA-transfected concentrations including the mock-transfected cells (transfected control). RSG at the concentration of 75 and 100 μM showed comparable results with the DMSO with both BiP siRNA and lamin A siRNA transfection (Figs. 7A and B).

D. 考察

The toxicological potential of TRO compared to that of another TZD agent, RSG, was investigated in a human hepatoma cell line, HepG2. In this study, TRO treatment showed concentration-dependent cytotoxicity with an approximate IC_{50} of 40 μM, whereas only a slight decrease in cell viability was found with RSG treatment (Fig. 1A). These results were consistent with the previous reports which additionally revealed that the lethal effects are exemplified by apoptosis (Bae et al., 2003; Bae and Song, 2003; Yamamoto et al., 2001). In this finding, the toxic effects of TRO in HepG2 cells were also exhibited in a time-dependent manner (Fig. 1B) and were significantly observed from 24 h of exposure. Although RSG showed a

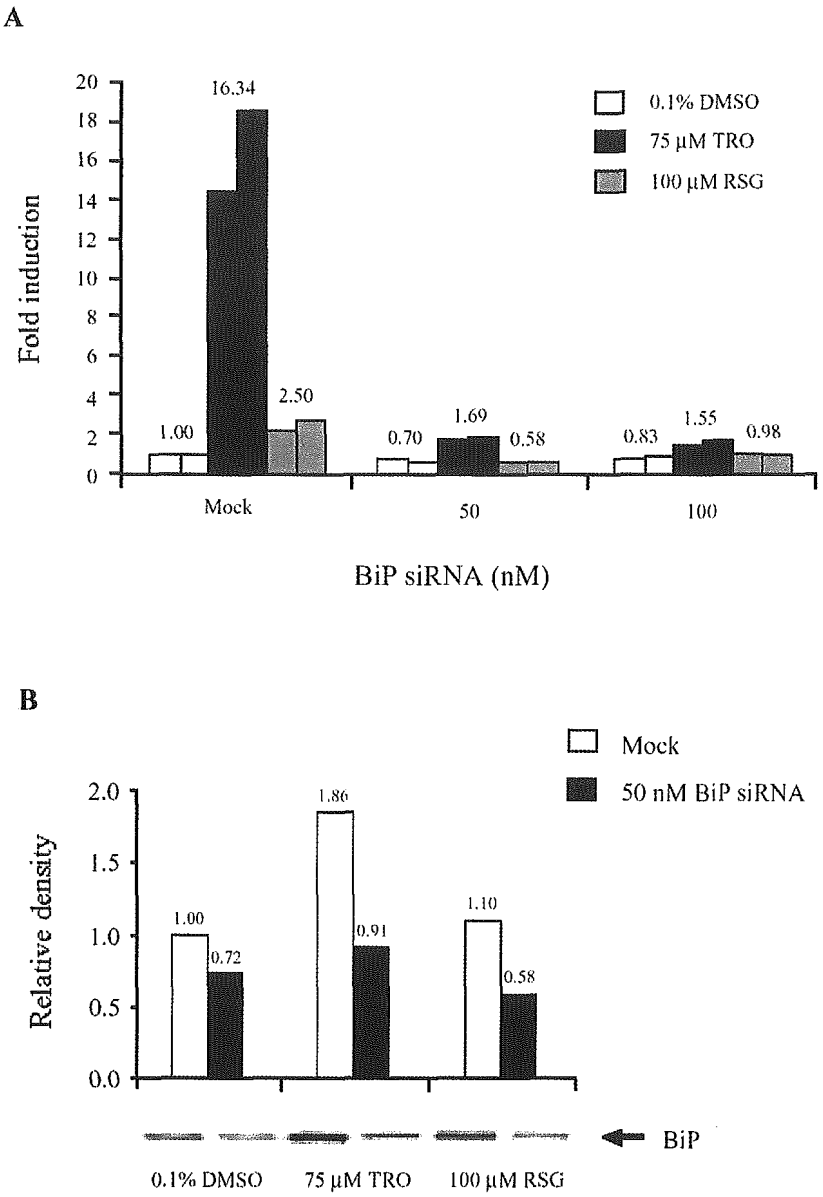

Fig. 6. Inhibitory effects of BiP siRNA on the BiP mRNA and protein expression. A, HLE cells were transfected with 50 or 100 nM of BiP siRNA for 24 h. TRO or RSG was added to the transfection medium to make a final concentration of 75 μM or 100 μM, respectively. DMSO (0.1%) treatment was used as a control. The cells were further incubated for 24 h. The cDNA was prepared for real-time PCR. Sense and antisense primers of BiP (5'-TGCTTGATGTATGTCCCCTTA-3' and 5'-CCTTGTCTTCAGCTGTCACT-3') were used. The relative BiP expression values were normalized with the GAPDH values of the same samples. B, HLE cells were transfected with 50 nM of BiP siRNA for 24 h. TRO or RSG was added to the transfection medium to make a final concentration of 75 μM or 100 μM, respectively. DMSO (0.1%) treatment was used as a control. The cells were further incubated for 24 h. The cell lysates were prepared and subjected to Western blotting with mouse anti-KDEL antibody for detecting BiP protein. The expression of BiP protein was measured using a densitometer. The data represent the average value of duplicate determinations.

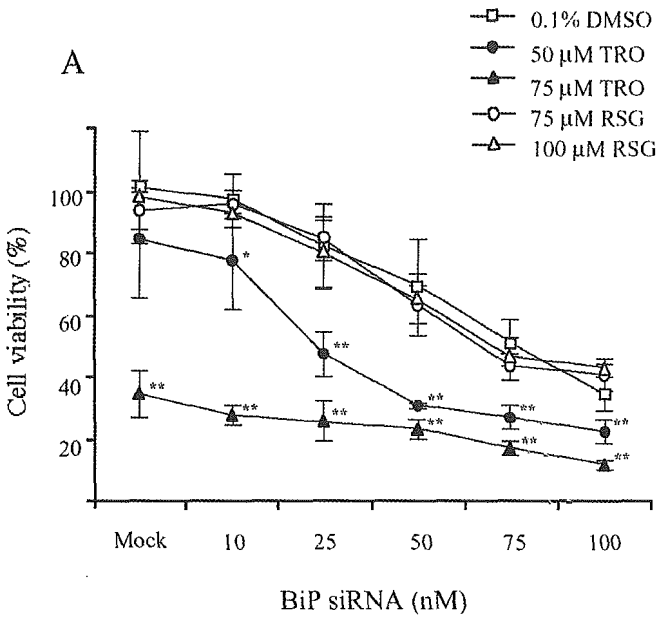

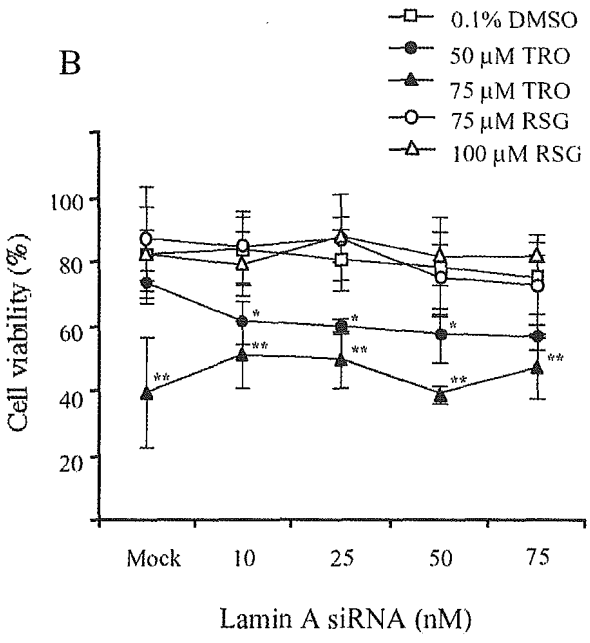

Fig. 7. Effects of BiP inhibition on cell viability. HLE cells were transfected with various concentrations of BiP siRNA (A) or lamin A siRNA as the negative control (B) for 24 h. TRO or RSG was added to the transfection medium to make a final concentration as indicated. DMSO (0.1%) treatment was used as a control. The cells were further incubated for 24 h. Cell viabilities were determined by ATP-based luminescent assay as described in Experimental Procedures. The cell viability values were calculated with cell viability of the non-treated cells as 100% (neither transfection reagent nor TZDs). The data represent the mean ± SD of at least three independent experiments. * $p < 0.05$, ** $p < 0.01$ compared with the control.

significant decrease in cell viability from 48 to 60 h ($p < 0.05$), percent cell viabilities were more than 80% of the control (Fig. 1B). The crystal violet assay could not be used to detect the time-dependent cytotoxicity because the cells did not adhere on the plate before 24 h after seeding. Confirming with the trypan blue exclusion assay from 4 to 60 h, the percent cell viabilities were comparable to those detected with crystal violet and significant lethal effects were observed from 12 to 60 h by 50 μM TRO (data not shown). TRO has been reported to be metabolized to three main metabolites: sulfate conjugated, glucuronide conjugated and quinone-type (TRO quinone) metabolites (Izumi et al., 1997a, b; Kawai et al., 1998). TRO, but not RSG, contains a 6-hydroxy-5,7,8-trimethylchromane moiety which undergoes metabolic activation by hepatic cytochrome P450 enzymes, CYP2C8 and CYP3A4, to generate TRO quinone (Yamazaki et al., 1999; Tettey et al., 2001). Based on the general involvement of quinones in cytotoxicity, TRO quinone has been reported to have a possible association with TRO-induced hepatotoxicity (Neuschwander-Tetri et al., 1998). Previously, a major epoxide of the quinone metabolite of TRO in HepG2 cells was found (Yamamoto et al., 2002). However, the toxicity possessed by either TRO quinone or the epoxide of TRO quinone is relatively lower than that of the parent compound (Tettey et al., 2001; Yamamoto et al., 2001, 2002). Thus, the hepatotoxic effects were more likely due to TRO or other unknown metabolites.

Since the remarkable cytotoxicity of TRO has been established, 2-DE was used to investigate the protein expression profiles of HepG2 cells treated with various concentrations of TRO or RSG. On 2-D gels, more than ten different spots according to the treatments were revealed (small part shown in Fig. 2). We focused on a spot of interest at an approximate MW of 75 kDa and isoelectric point of 5.0 which showed distinct dose-dependency and TRO-specific changes with the greatest expression. The protein spot was highly matched with BiP and also, to a lesser extent, PDIrp (Fig. 3). These proteins are recognized as chaperone proteins that reside in the ER.

BiP, known as a 78 kDa glucose-regulated protein (Grp78), is related to the highly conserved 70 kDa heat shock protein (hsp70) family (Munro and Pelham, 1986). Apart from its response to heat, BiP is also the best-characterized chaperone, and is abundantly and constitutively expressed in the ER of all eukaryotic cells (Haas, 1994). This protein is responsible for normal cellular functions such as assisting protein folding, assembly and disassembly for maintenance as well as the degradation of untenable proteins. BiP production can be induced by various perturbations of ER functions such as the expression of mutant proteins or protein subunits, reductive stress, ER Ca^{2+} depletion and the inhibition of asparagine (N)-linked glycosylation (Gething and Sambrook, 1992; Haas, 1994; Kaufman, 1999, Lee, 2001). In this study, TRO treatment elicited a dose-

dependent overexpression of BiP protein as confirmed by Western blotting (Fig. 4A). BiP mRNA was also induced by treatment with 50 and 75 μM of TRO (Fig. 5A). At 100 μM TRO treatment, which resulted in about 15% cell viability, the highest induction of BiP protein was observed, but not the mRNA. Gülow et al. (2002) reported that under ER stress conditions, BiP expression is tightly controlled post-transcriptionally, allowing the cells to produce more proteins which are independent from the transcription level. As shown in Fig. 6B, with the inhibition of BiP mRNA expression before TRO or RSG treatment, the induction of BiP protein could not be achieved. Thus, the effects of 100 μM TRO treatment could be in part explained by the high translation efficiency of BiP protein in HepG2 cells. In this observation, RSG treated HepG2 cells also induced BiP expression but at a low level, which would account for its lower toxicity compared to TRO.

Protein disulfide isomerase related protein (herein referred to as PDIrp), or 72 kDa endoplasmic reticulum protein (ERp72), is also a resident chaperone in the ER which shares amino acid sequences with ERp59 (PDI) and holds three copies of the thioredoxin active unit (Gething and Sambrook, 1992; Mazzarella et al., 1990). In normal cells, PDIrp is expressed constitutively at low levels and is induced by the same treatments that affect BiP expression (Huang et al., 1989). PDIrp was found close to the BiP spot. However, unlike BiP, PDIrp protein was expressed equally in all treatments (Fig. 4B). Given the similar characteristics between PDIrp and PDI (Mazzarella et al., 1990), the PDI protein level was also investigated in the same set of treated samples using its specific antibody. Indeed, the PDI protein expression showed comparable results (Fig. 4C) to PDIrp. Although a small induction of PDIrp mRNA was observed at the high doses of 75 and 100 μM, neither treatments lead to the overproduction of the protein. These present data suggest that the damage caused by TRO treatment was unlikely related to the increased PDI.

In order to confirm the prominent regulation of BiP by TRO-induced cytotoxicity, the RNA interference method was applied to HLE, another human hepatoma cell line. In the condition of siRNA transfection with TRO treatment, BiP expression was suppressed by about 90% compared to the corresponding mock-transfected cells (Fig. 6A). This finding was reflected by the phenotypic change in cell viability. TRO caused changes in the permeability and structure of mitochondria as well as a depletion of ATP, which were correlated with the decrease of cell viability (Tirmenstein et al., 2002). With a small amount of cells, the luminescent assay was considered to be sufficiently sensitive to detect the relative ATP (Fig. 1C) and showed parallel results with the cell viability in Fig. 1A. Thus, to observe the phenotypic changes caused by the TRO-induced suppression of BiP, ATP produced by metabolically active

cells was used as a biomarker in this study. Comparing the results in Figs. 7A and B, it was found that the inhibition of BiP appeared to promote cell death even in the absence of TRO. This supports the crucial function of BiP in normal cellular processes (Gething and Sambrook, 1992; Haas, 1994; Kaufman, 1999). Doses of 50 and 75 μM TRO as well as 75 and 100 μM RSG, which caused the high levels of BiP mRNA expression, were used. Interestingly, in the presence of 50 μM TRO, the inhibition of BiP expression rendered cells more susceptible to the lethality as demonstrated by a gradual increase in significant cell toxicity along with the increase in the concentration of BiP siRNA (Fig. 7A). Supporting this finding, a related study reported that inhibition of BiP synthesis sensitizes cells to oxidative stress (Liu et al., 1998). These phenotypic changes in cell viability suggested the crucial role of BiP overexpression in the effects of TRO exposure.

It is well known that ER is a major cellular storage site of Ca^{2+} in the cell, and ER chaperones also play important roles in Ca^{2+} accumulation and release. Both BiP and PDIrp are Ca^{2+}-binding proteins (Lee, 2001). Any disturbance in the ER homeostasis causes a release of Ca^{2+} which in turn blocks ER protein processing, resulting in the accumulation of incompletely folded proteins, and activates the transcription of ER chaperone genes including *BiP* (Liu et al., 1998; Lodish and Kong, 1990). In previous reports, TRO but not RSG exhibited antiproliferative effects on cultured cells via a depletion of Ca^{2+} from the storage site that results in the inhibition of translation initiation (Fan et al., 2004; Palakurthi et al., 2001). Together with these results, it might be postulated that TRO acts as a chemical signal that causes the release of Ca^{2+} from the ER, and that BiP expression is one of the cellular responses induced by TRO toxicity. In addition, the effects of TRO on the activation of JNK pathway (Bae and Song, 2003), disturbance of mitochondria function and depletion of ATP (Tirmenstein et al., 2002) may also converge in the ER stress response (Breckenridge et al., 2003).

E. 結論

The possibility was raised in the present study that the ER is one of the targets involved in TRO hepatotoxicity. TRO may serve as a stress signal to the ER, which in turn, causes the overproduction of BiP in response to cytotoxicity. Supporting this view, the inhibition of BiP at the post-transcriptional level sensitized the cells to lethality.

F. 研究発表

1. 論文発表

Maniratanachote R, Minami K, Katoh M, Nakajima M, and Yokoi T.(2005) Chaperone proteins involved in troglitazone-induced toxicity in human hepatoma cell lines. *Toxicol. Sci.* 83, 293-302.

2. 学会発表

Yokoi, T., Mechanistic approach to drug induced idiosyncratic hepatotoxicity, 1st Indo-Japanese International Conference on Advances in Pharmaceutical Research and Technology 11. 25-29, Mumbai, India (2005).

Yokoi, T., Idiosyncratic drug reactions and pharmacogenetics: The troglitazone case. Symposium for Mechanism of Adverse Drug Reactions. 13th North-America ISSX and 20th JSSX joint meeting, 10. 23-27, Hawaii, USA (2005).

G. 知的財産権の出願・登録状況

なし

H. 参考論文

Bae, M. A., and Song, B. J. (2003). Critical role of c-Jun N-terminal protein kinase activation in troglitazone-induced apoptosis of human HepG2 hepatoma cells. *Mol. Pharmacol.* 63, 401-408.

Bae, M. A., Rhee, H., and Song, B. J. (2003). Troglitazone but not rosiglitazone induces G1 cell cycle arrest and apoptosis in human and rat hepatoma cell lines. *Toxicol. Lett.* 139, 67-75.

Breckenridge, D. G., Germain, M., Mathai, J. P., Nguyen, M., and Shore, G. C. (2003). Regulation of apoptosis by endoplasmic reticulum pathways. *Oncogene* 22, 8608-8618.

Fan, Y. H., Chen, H., Natarajan, A., Guo, Y., Harbinski, F., Iyasere, J., Christ, W., Aktas, H., and Halperin, J. A. (2004). Structure-activity requirements for the antiproliferative effect of troglitazone derivatives mediated by depletion of intracellular calcium. *Bio. Med. Chem. Lett.* 14, 2547-2550.

Freid, J., Everitt, D., and Boscia, J. (2000). Rosiglitazone and hepatic failure. *Ann. Inter. Med.* 132, 164.

Fujiwara, T., Yoshioka, S., Yoshioka, T., Ushiyama, I., and Horikoshi, H. (1988). Characterization of new oral antidiabetic agent CS-045: Studies in KK and ob/ob mice and Zucker fatty rats. *Diabetes* 37, 1549-1558.

Gitlin N, Julie, N. L., Spurr, C. L., Lim, K. N., and Juarbe, H. M. (1998). Two cases of severe clinical and histologic hepatotoxicity associated with troglitazone. *Ann. Intern. Med.* 129, 36-38.

Gülow, K., Bienert, D., and Haas, I. G. (2002). BiP is feed-back regulated by control of protein translation efficiency. *J. Cell Sci.* 115, 2443-2452.

Haas, I. G. (1994). BiP (GRP78), an essential hsp70 resident protein in the endoplasmic reticulum. *Experientia* 50, 1012-1020.

Huang, S. H., Tomich, J. M., Wu, H., Jong, A., and Holcenberg, J. (1989). Human deoxycystidine kinase, sequence of cDNA

clones and analysis of expression in cell lines with and without enzyme activity. *J. Biol. Chem.* 264, 14762-14768. Erratum in: *J. Biol. Chem.* 266, 5353.

Isley, W. L., and Oki, J. C. (2000). Rosiglitazone and liver failure. *Ann. Intern. Med.* 133, 393.

Izumi, T., Enomoto, S., Hoshiyama, K., Sasahara, K., and Sugiyama, Y. (1997a). Pharmacokinetic stereoselectivity of troglitazone, an antidiabetic agent, in the KK mouse. *Biopharm. Drug Dispos.* 18, 305-324.

Izumi, T., Hoshiyama, K., Enomoto, S., Sasahara, K., and Sugiyama, Y. (1997b). Pharmacokinetics of troglitazone, an antidiabetic agent: Prediction of in vivo stereoselective sulfation and glucuronidation from in vitro data. *J. Pharmacol. Exp. Ther.* 280, 1392-1400.

Kaufman, R. J. (1999). Stress signaling from the lumen of the endoplasmic reticulum: Coordination of gene transcriptional and translational control. *Genes & Dev.* 13, 1211-1233.

Kawai, K., Odaka, T., Tsurata, F., Tokui, T., Ikeda, T., and Nakamura, K. (1998). Stereoselective metabolism of new oral anti-diabetic agent troglitazone stereoisomers in liver. *Xenobio. Metab. Dispos.* 13, 362-368.

Lebovitz, H. E., Kreider, M., and Freed, M. I. (2002). Evaluation of liver function in type 2 diabetic patients during clinical trials. *Diabetes Care* 25, 815-821.

Lee, A. S. (2001). The glucose-regulated proteins: Stress induction and clinical applications. *Trends Biochem. Sci.* 26, 504-510.

Lehmann, J. M., Moore, L. B., Smith-Oliver, T. A., Wilkison, W. O., Willson, T., and Kliewer, S. A. (1995). An antidiabetic thiazolidinedione is a high affinity ligand for peroxisome-activated receptor g (PPARg). *J. Biol. Chem.* 270, 12953-12956.

Liu, H., Miller, E., van de Water, B., and Stevens, J. L. (1998). Endoplasmic reticulum stress proteins block oxidant-induced Ca^{2+} increases and cell death. *J. Biol. Chem.* 273, 12858-12862.

Lodish, H. F., and Kong, N. (1990). Perturbation of cellular calcium blocks exit of secretory proteins from the rough endoplasmic reticulum. *J. Biol. Chem.* 265, 10893-10899.

Lowry, O. H., Rosebrough. N. J., Farr, A. L., and Randall, R. J. (1951). Protein measurement with the Folin phenol reagent. *J. Biol. Chem.* 193, 265-275.

Mazzarella, R. A., Srinivasan, M., Haugejorden, S. M., and Green, M. (1990).

ERp72, an abundant luminal endoplasmic reticulum protein, contains three copies of the active site sequences of protein disulfide isomerase. *J. Biol. Chem.* 265, 1094-1101.

Neuschwander-Tetri, B. A., Isley, W. L., Oki, J. C., Ramrakhiani, S., Quiason, S. G., Phillips, N. J., and Brunt, E. M. (1998). Troglitazone-induced hepatic failure leading to liver transplantation. *Ann. Intern. Med.* 129, 38-41.

Nolan, J. J., Ludvik, B., Beerdsen, P., Joyce, M., and Olefsky, J. (1994). Improvement in glucose tolerance and insulin resistance in obese subjects treated with troglitazone. *N. Engl. J. Med.* 331, 1188-1193.

O'Farrell, P. H. (1975). High resolution two-dimensional electrophoresis. *J. Biol. Chem.* 250, 4007-4021.

Palakurthi, S. S., Aktas, H., Grubissich, L. M., Mortensen, R. M., and Halperin, J. A. (2001). Anticancer effects of thiazolidinediones are independent of peroxisome proliferators-activated receptor g and mediated by inhibition of translation initiation. *Cancer Res.* 61, 6213-6218.

Rothwell, C., McGuire, E. J., Altrogge, D. M., Masuda, H., and de la Iglesia, F. A. (2002). Chronic toxicity in monkeys with the thiazolidinedione antidiabetic agent troglitazone. *J. Toxicol. Sci.* 27, 35-47.

Shibuya, A., Watanabe, M., Fujita, Y., Saigenji, K., Kuwao, S., Takahashi, H., and Takeuchi, H. (1998). An autopsy case of troglitazone-induced fulminant hepatitis. *Diabetes Care* 21, 2140-2143.

Tettey, J. N., Maggs, J. L., Rapeport, W. G., Pirmohamed, M., and Park, B. K. (2001). Enzyme induction dependent bioactivation of troglitazone and troglitazone quinone in vivo. *Chem. Res. Toxicol.* 14, 965-974.

Tirmenstein, M. A., Hu, C. X., Gales, T. L., Maleeff, B. E., Narayanan, P. K., Kurali, E., Hart, T. K., Thomas, H. C., and Schwartz, L. W. (2002). Effects of troglitazone on HepG2 viability and mitochondrial function. *Toxicol. Sci.* 69, 131-138.

Watanabe, T., Ohashi, Y., Yasuda, M., Takaoka, M., Furukawa, T., Yamoto, T., Sanbuissho, A., and Manabe, S. (1999). Was it possible to predict liver dysfunction caused by troglitazone during the nonclinical safety studies? *Iyakuhin Kenkyu* 30, 537-546.

Yamamoto, Y., Nakajima, M., Yamazaki, H., and Yokoi, T. (2001). Cytotoxicity and apoptosis produced by troglitazone in human hepatoma cells. *Life Sci.* 70, 471-482.

Yamamoto, Y., Yamazaki, H., Ikeda, T., Watanabe, T., Iwabuchi, H., Nakajima, M., and Yokoi, T. (2002). Formation of a quinone epoxide metabolite of troglitazone with

cytotoxic to HepG2 cells. *Drug Metab. Dispos.* 30, 155-160.

Yamazaki, H., Shibata, A., Suzuki, M., Nakajima, M., Shimada N., Guengerich, F. P., and Yokoi, T. (1999). Oxidation of troglitazone to a quinone-type metabolite catalyzed by cytochrome P-450 2C8 and P-450 3A4 in human liver microsomes. *Drug Metab. Dispos.* 27, 1260-1266.